J. Indian Chem. Soc.,
Vol. 94, November 2017, pp. 1163-1172

Induced CD from chiral Schiff base metal complexes involving azo-dye groups to gold nanoparticles

Yuki Tsutsumi, Nobumitsu Sunaga, Tomoyuki Haraguchi and Takashiro Akitsu*

Department of Chemistry, Faculty of Science, Tokyo University of Science, 1-3 Kagurazaka, Shinjuku-ku, Tokyo 162-8601, Japan

E-mail : akitsu@rs.kagu.tus.ac.jp *Fax* : 81-3-5261-4631

Manuscript received 02 October 2017, revised 12 November 2017, accepted 14 November 2017

Abstract : We reported on synthesis, characterization, and docking of supramolecular systems of azo-group containing chiral salen-type Schiff base Ni^{II}, Cu^{II} and Zn^{II} complexes and colloidal gold nanoparticles (AuNPs) of 10 nm diameters. Appropriate conditions enabled some of them to exhibit induced CD from chiral species adsorbed on the surface of AuNPs. We have compared differences of dipole-dipole interactions of *cis-trans* isomerization as well as coordination geometries of these complexes associated with induce CD spectra around plasmon region. This optical features will be promising light absorption mechanism of dyes for solar cells developing new concept of organic/inorganic hybrid functional materials.

Keywords : Chirality, azobenzene, Schiff base complexes, gold nanoparticles, TD-DFT.

Introduction

In recent years, organic/inorganic hybrid materials of nanoparticles (such as metal clusters[1] or semiconductors[2]) and chiral (biochemical[3], organic[4] and metal complex[5,6]) molecules have been widely investigated. For example, nano-scaled hybrid catalysts may have two approach, to have chiral ligands on the surface or to have chiral catalysts[7], microchips[8] or electronically-tuned quantum dots[9]. However, direct adsorption of chiral metal complexes onto metal nanoparticles has been reported from the viewpoint of their optical properties.

Mechanisms of induced CD of nanoparticles (surface plasmon region, if possible) from chiral adsorbed molecules were well understood theoretically, which was concluded properly oriented dipole-dipole interaction mainly[10–12]. Surface plasmon resonance is the resonant oscillation of conduction electrons at the interface (of AuNPs) between negative and positive permittivity material stimulated by incident light, which exhibits characteristic color depending on size of AuNPs. Previously, we have also reported some hybrid systems of chiral metal complexes to investigate induced CD[5], though limited cases could indicate induced CD or related phenomenon actually because of restriction of molecular orientation or other conditions[13]. Depending on molecular shape of chiral metal complexes, disappearance of CD bands was observed merely[6]. However, we have also studied on Weigert effect using azobenzene and related dyes with hybrid dopants of chiral metal complexes in polymer films media[14–16]. By combination of two techniques, we can control molecular orientation of chiral and having azobenzene dyes (metal complexes) and intentionally inducing CD bands around plasmon region as a concept. However, no study was carried out actually. Such additional light absorption may be applied for materials of solar cells[17,18].

Herein, we have newly prepared three *'chiral'* Schiff base metal complexes having azobenzene moiety in their ligands (Fig. 1). After evaluation of their optical properties by TD-DFT computations, we measured induced CD bands by mixing AuNPs dispersions experimentally. Furthermore, we also irradi-

ated linearly polarized light UV light (< 350 nm) expecting not only *trans-cis* photoisomerization of azobenzene moiety but also rotation of molecular orientation of azo-complexes due to Weigert effect and discuss the changes of induced CD bands for three different chiral complexes.

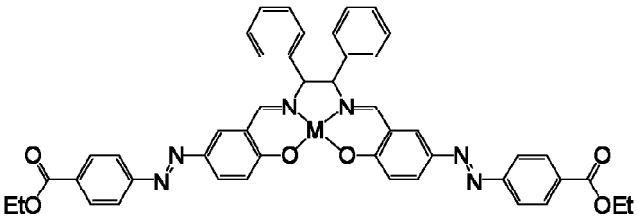

Fig. 1. Molecular structures of **NiAZ** (M=Ni), **CuAZ** (M=Cu) and **ZnAZ** (M=Zn).

Experimental

General procedures :

Chemicals of the highest commercial grade available (10 nm gold nanoparticles BMGC10 from Funakoshi, solvents from Kanto Chemical, organic compounds from Tokyo Chemical Industry and metal sources from Wako) were used as received without further purification. Ethylacetylazobenzenesalycylaldehyde was prepared in a similar procedure to the analogous compounds[19]. Solutions (0.01 mM) of complex : gold nanoparticles = 1 : 1 (v/v) were used for spectral measurements.

Preparation of complexes :

To a solution of ethylmethylazobenzenesalycylaldehyde (0.59658 g, 2.00 mmol) dissolved in methanol (40 mL), (1*R*,2*R*) -(+)-1,2-diphenylethylenediamine (0.2122 g, 1.00 mmol) was added and stirred at 313 K for 2 h to give yellow solution of ligand. nickel(II) acetate tetrahydrate (0.1244 g, 0.50 mmol), copper(II) acetate monohydrate (0.1996 g, 1.00 mmol), or zinc(II) acetate dehydrate (0.2195 g, 1.00 mmol) was added to the resulting solution and stirring at 313 K for 2 h to give yellow, green, or yellow solutions of **NiAZ**, **CuAZ**, or **ZnAZ**, respectively. After cooling the solutions, compounds were filtered.

NiAZ : Yield 0.089 g (54.64%). Anal. Found : C, 65.68; H, 5.08; N, 9.38%. Calcd. for $C_{46}H_{38}N_6NiO_6$: C, 66.60; H, 4.62; N, 10.13%; IR (KBr (cm^{-1})) : 403, 410, 431, 447, 471, 506, 544, 567, 574, 579, 663, 1118, 1143, 1275, 1543, 1548, 1557, 1588 (N=N), 1603, 1628 (C=N), 1683, 1704, 1716, 2874, 2929, 2952; UV-Vis (diffuse reflectance (nm)) 430 (CT) and 573 (d-d); CD (KBr) 409 (CT) and 572 (d-d).

CuAZ : Yield 0.3060 g (43.67%). Anal. Found : C,64.06; H, 4.79; N, 9.93%. Calcd. for $C_{46}H_{38}N_6CuO_6$: C, 66.22; H, 4.59; N, 10.07%; IR (KBr (cm^{-1})) : 400, 412, 420, 426, 433, 445, 457, 490, 520, 526, 574, 581, 595, 665, 673, 699, 771, 857, 1016, 1036, 1125, 1143, 1245, 1273, 1334, 1381, 1458, 1588, 1601 (N=N), 1630 (C=N), 1700, 1717, 2361, 2370, 2454, 2849, 2930, 2984; UV-Vis (diffuse reflectance (nm)) 399 (CT) and 582 (d-d); CD (KBr) 379 (CT) and 575 (d-d).

ZnAZ : Yield 0.3060 g (43.67%). 0.2036 g (56.89%). Anal. Found : C, 65.92; H, 4.67; N, 9.86%. Calcd. for $C_{46}H_{38}N_6ZnO_6$: C, 66.07; H, 4.58; N, 10.07%; IR (KBr (cm^{-1})) : 403, 407, 417, 425, 440, 450, 469, 481, 501, 522, 534, 569, 572, 584, 636, 770, 855, 1107, 1187, 1277, 1329, 1379, 1592 (N=N), 1601, 1631, 1636 (C=N), 1716, 1791, 1916, 2361, 2496, 2539, 2671, 2695, 2873, 2932, 2992; UV-Vis (diffuse reflectance (nm)) 404 (CT). CD (KBr) 401 (CT).

Physical measurements :

Elemental analyses (C, H, N) were carried out with a Perkin-Elmer 2400II CHNS/O analyzer at Tokyo University of Science. Infrared spectra were recorded as KBr pellets on a JASCO FT-IR 4200 plus spectrophotometer in the range of 4000–400 cm^{-1} at 298 K. Electronic spectra were measured on a JASCO V-570 UV/VIS/NIR spectrophotometer (equipped with an integrating sphere for diffuse reflectance spectra) in the range of 800–200 nm at 298 K. Circular dichroism (CD) spectra were measured as KBr pellets on a JASCO J-820 spectropolarimeter in the range of 800–

200 nm at 298 K. Photo-illumination were carried out using a lamp (1.0 mW/cm^2) with optical filters (UV λ = 200–400 nm) leading to a sample by using optical fibers and polarizer through optical filters. The powder X-ray diffraction patterns were measured on a Rigaku Smart Lab (CuKα radiation) at 2θ = 5–60 deg, step width 0.01 deg, scan speed 0.3 deg/min, capillary diameter 0.3 mm. Structural analysis by the Rietveld method was carried out using PDXL2 ver.2.2.1.0 (Rigaku Corporation).

NiAZ (CCDC 1572657) : $C_{46}H_{38}N_6NiO_6$, M_w = 829.52, monoclinic, $P2_1$ (#4), a = 23.82(3) Å, b = 15.27(3) Å, c = 21.075(19) Å, β = 109.20(6)°, V = 7239(17) Å^3, Z = 2, R_{wp} = 0.0968.

CuAZ (CCDC 1572666) : $C_{46}H_{38}N_6CuO_6$, M_w = 829.524, triclinic, $P1$ (#1), a = 14.20(3) Å, b = 36.96(14) Å, c = 13.85(4) Å, α = 90.0(2)°, β = 99.7(2)°, γ = 96.17(16)°, V = 7118(37) Å^3, Z = 1, R_{wp} = 0.0678.

ZnAZ (CCDC 1572669) : $C_{46}H_{38}N_6ZnO_6$, M_w = 836.24, monoclinic, $P2_1$ (#4), a = 21.63(3) Å, b = 21.75(12) Å, c = 18.5(2) Å, β = 103.41(17)°, V = 8463(104) Å^3, Z = 2, R_{wp} = 0.0310.

Computational methods :

All calculations were performed using the Gaussian 09W software Revision D.01 (Gaussian, Inc.)[20]. The gas phase geometry optimizations were carried out using TD-DFT with B3LYP functional. The vertical excitation energy was calculated with the Lanl2dz for Ni, Cu, and Zn with the 6-31+G(d) basis set for H, C, N, and O method based on the singlet ground state geometry.

Results and discussion

Crystal structures :

The molecular structures of **NiAZ**, **CuAZ**, and **ZnAZ**, determined with Rietveld analysis are depicted in Figs. 2–4, respectively. In the solid state, **NiAZ**,

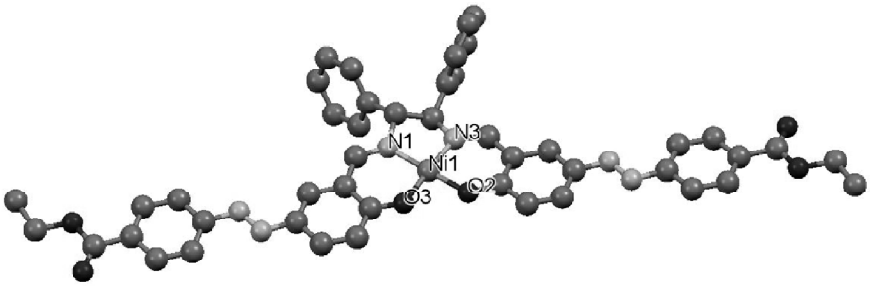

Fig. 2. Crystal structure of **NiAZ**. Selected bond lengths (Å) and angles (°) : Ni1-O2 = 1.766(3), Ni1-O3 = 1.795(14), Ni1-N1 = 1.791(2), Ni1-N3 = 1.8257(14), O2-Ni1-O3 = 83.80(11), O2-Ni1-N1 = 177.654(4), O2-Ni1-N3 = 95.85(11), O3-Ni1-N1 = 95.47(10), O3-Ni1-N3 = 177.548(3), N1-Ni1-N3 = 85.24(10).

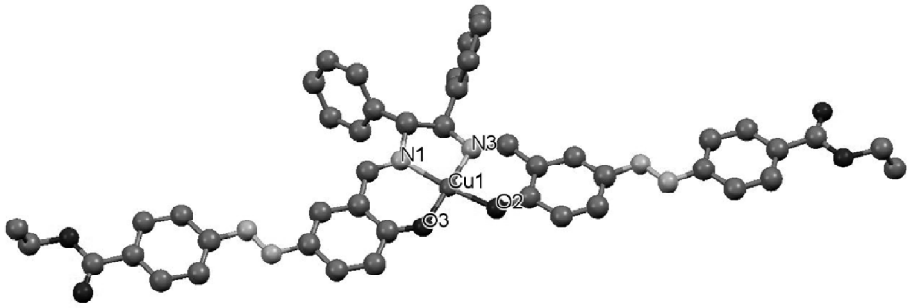

Fig. 3. Crystal structure of **CuAZ**. Selected bond lengths (Å) and angles (°) : Cu1-O2 = 2.057(5), Cu1-O3 = 1.929(6), Cu1-N1 = 2.121(6), Cu1-N3 = 1.971(6), O2-Cu1-O3 = 91.1(2), O2-Cu1-N1 = 173.35(2), O2-Cu1-N3 = 92.9(2), O3-Cu1-N1 = 93.0(2), O3-Cu1-N3 = 173.06(3), N1-Cu1-N3 = 83.6(2).

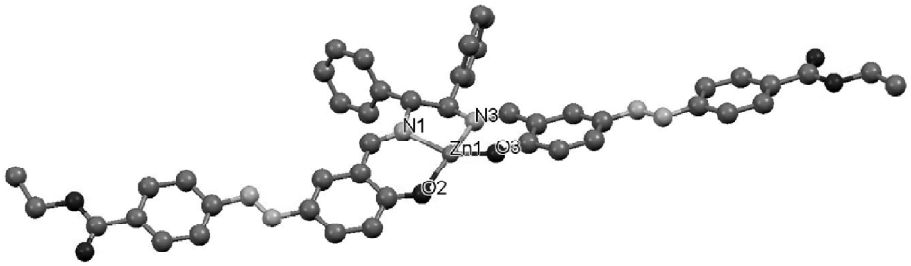

Fig. 4. Crystal structure of **ZnAZ**. Selected bond lengths (Å) and angles (°) : Cu1-O2 = 2.057(5), Cu1-O3 = 1.929(6), Cu1-N1 = 2.121(6), Cu1-N3 = 1.971(6), O2-Cu1-O3 = 91.1(2), O2-Cu1-N1 = 173.35(2), O2-Cu1-N3 = 92.9(2), O3-Cu1-N1 = 93.0(2), O3-Cu1-N3 = 173.06(3), N1-Cu1-N3 = 83.6(2).

CuAZ, and **ZnAZ** afford four-coordinated square planar *trans*-[NiN_2O_2], distorted square planar *trans*-[CuN_2O_2], and compressed tetrahedral *trans*-[ZnN_2O_2], respectively. Two phenyl groups derived from diamine moiety took a characteristic conformation to reduce steric repulsion due to hindrance between large groups. Beside them (namely phenyl groups and coordination environment), most part of conjugate ligands were located in a plane. As a stable structure, azobenzene moiety of all complexes were found to be *trans*-conformation. All geometries are within normal ranges of values for the analogous Schiff base metal complexes[21–24].

TD-DFT computation :

Besides crystal structures determined, we also examined optimized structures of these metal complexes as both *cis* and *trans* forms and estimated their electronic properties (dipole moments and simulated UV-Vis and CD spectra) based on TD-DFT calculations. Figs. 5–7 depicted optimized structures with transition moments for **NiAZ**, **CuAZ** and **ZnAZ**, respectively. The TD-DFT simulated UV-Vis and CD spectra corresponding to the optimized structures are shown in Figs. S1–S3, respectively. Sterically, all optimized structures of the *trans* forms were similar to that of crystal structure, of which planar moieties in the ligands connected to keep planarity. Although the lack of appropriate substituent groups to coordinate AuNPs in this ligand, weak intermolecular interaction to fit surface must be important factor to emerge induced CD in discussion elsewhere[25]. In this case, molecular shape may be the most important factor. Electronically, in contrast, the largest magnitude of transition moments (in *trans* forms) of **CuAZ** may ascribed to asymmetry of optimized coordination geometries and extension of identical polar ligands from

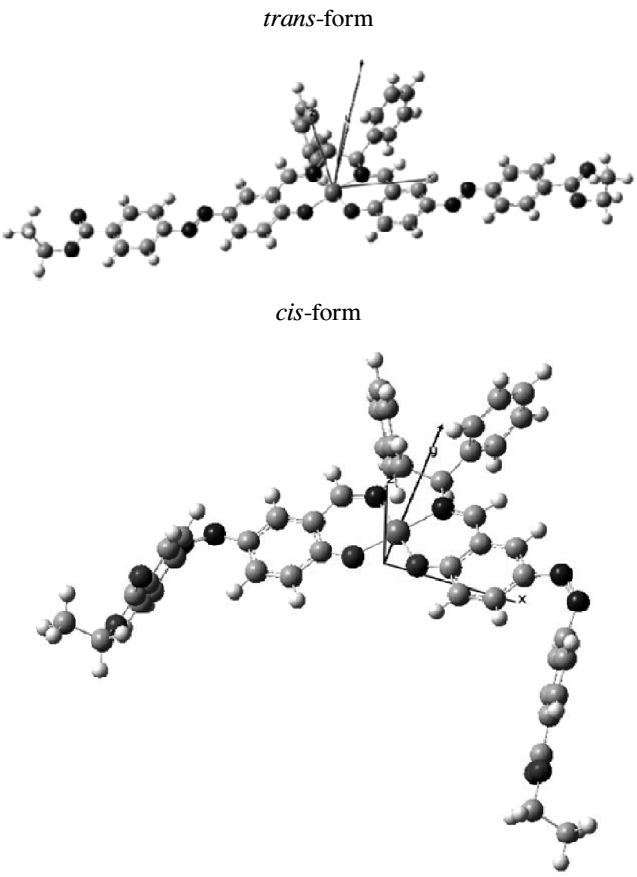

Fig. 5. Optimized structures by means of TD-DFT of *trans* (above) and *cis* (below) forms of **NiAZ**. The arrow denotes direction of dipole moments : *trans* (0.3674, 5.3136, 0.3948; 5.3408 Debye), *cis* (0.0000, 6.5037, 0.0000; 6.5037 Debye).

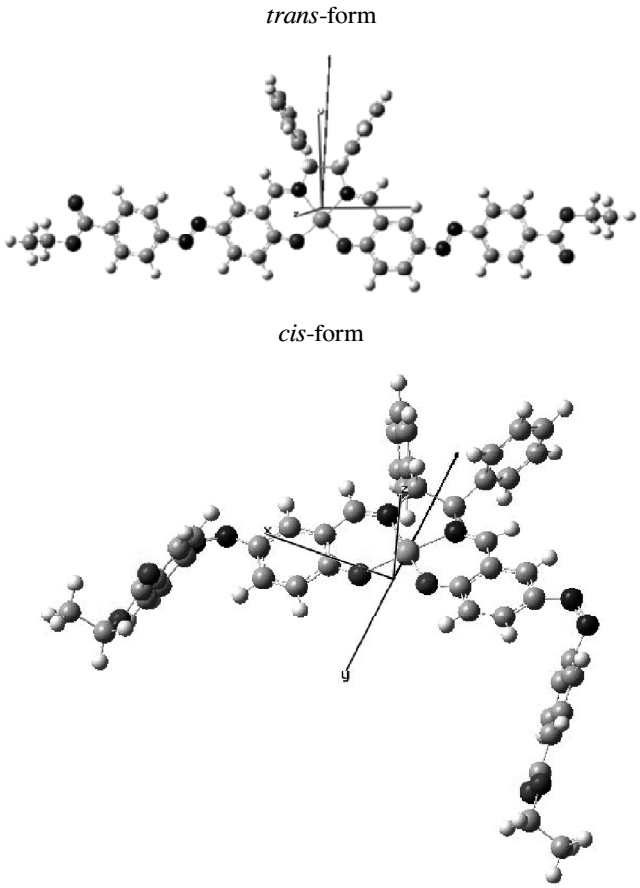

Fig. 6. Optimized structures by means of TD-DFT of *trans* (above) and *cis* (below) forms of **CuAZ**. The arrow denotes direction of dipole moments : *trans* (0.6467, 8.2497, –0.2080; 6.4097 Debye), *cis* (0.0001, –6.4097, 0.0001; 8.2778 Debye).

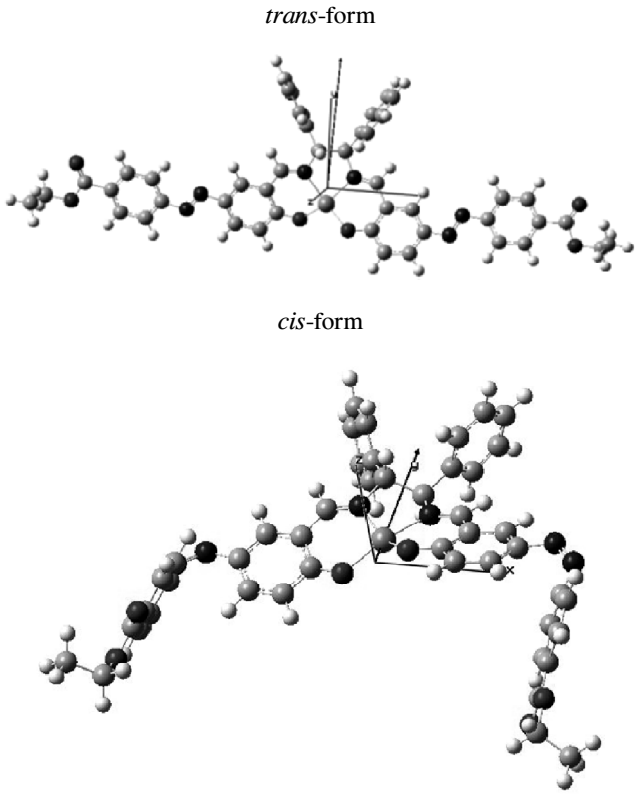

Fig. 7. Optimized structures by means of TD-DFT of *trans* (above) and *cis* (below) forms of **ZnAZ**. The arrow denotes direction of dipole moments : *trans* (0.3467, 4.4637, 0.4083; 4.4958 Debye), *cis* (–0.0002, 6.1555, 0.0001; 6.1555 Debye).

the central metal moieties. For all complexes, the *cis* forms indicated larger values of dipole moments than that of the *cis* forms, which is attributed to localization of polar moieties in the ligands[26]. Although the direction of dipole moment was changed (from parallel to perpendicular against diphenyl groups) for **NiAZ** and **CuAZ** after photoisomerization of azo-groups (from *trans* to *cis*) in the ligands, **ZnAZ** did not change (and kept parallel as the expression above). This differences are attributed from characteristic compressed tetrahedral coordination geometry of **ZnAZ**.

UV-Vis and CD spectra :

At first, UV-Vis and CD spectra of 0.01 mM methanol solutions of each complex, 0.02 mM methanol dispersion of AuNPs were measured for observation of optical or chiroptical properties of sole components. Next, after mixing these complexes and AuNPs dispersions, UV-Vis and the corresponding CD spectra of them were also measured for detection of induced CD as prepared in other words, as the *trans* form, dipole moments of complexes and AuNPs (of which dipole moments along the direction of vertical line of the surface). Finally, after linearly polarized UV light irradiation for 5 min, UV-Vis and CD spectra of the mixed dispersions were also measured after standing for 30 min to observe the effect of *cis-trans* photoisomerization of azo groups in the ligands (as estimated spectral and dipole moment changes by means TD-DFT calculations) and the possibility of so-called Weigert effect on the surface of AuNPs. Weigert effect may induce anisotropic molecular align-

ment of molecular dipole moment (in many cases, long axis of molecules having azobenzene moiety) perpendicular to electric vectors of linearly polarized UV light. Weigert effect can be occurred only by irradiation of linearly polarized UV light, though *cis-trans* photoisomerization of azo groups can be occurred by irradiation UV light merely (and even within less than 3 min generally).

Figs. 8–10 show CD and UV-Vis and CD spectra of **NiAZ**, **CuAZ**, and **ZnAZ** and/or AuNPs before and after UV light irradiation up to 5 min, respectively. For **NiAZ** system (Fig. 8), before UV light irradiation, it should be noted that mixed dispersions of the complex and AuNPs exhibit predominantly positive induced CD bands at about 500 nm. After UV light irradiation, it should be noted that mixed dispersions of the complex and AuNPs exhibit predominantly positive induced CD bands at about 500 nm. Additionally, after 30 min, it should be noted that mixed dispersions of the complex and AuNPs exhibit predominantly negative induced CD bands at about 500 nm. The bands are close to surface plasmon band of AuNPs[5,25].

For **CuAZ** system (Fig. 9), before UV light irradiation, it should be noted that mixed dispersions of the complex and AuNPs exhibits predominantly positive induced CD bands at about 550 nm. After UV light irradiation, it should be noted that mixed dispersions of the complex and AuNPs exhibit predominantly positive induced CD bands at about 500–600 nm. Additionally, after 30 min, it should be noted that mixed dispersions of the complex and AuNPs exhibit predominantly negative induced CD bands at about 500–600 nm. The bands are close to surface plasmon band of AuNPs. Consequently, it suspected that they appeared negative induced CD bands by UV irradiation[6].

For **ZnAZ** (Fig. 10), before UV light irradiation, it should be noted that mixed dispersions of the complex and AuNPs exhibit predominantly positive induced CD bands at about 500 nm. After UV light irradiation, it should be noted that mixed solutions of

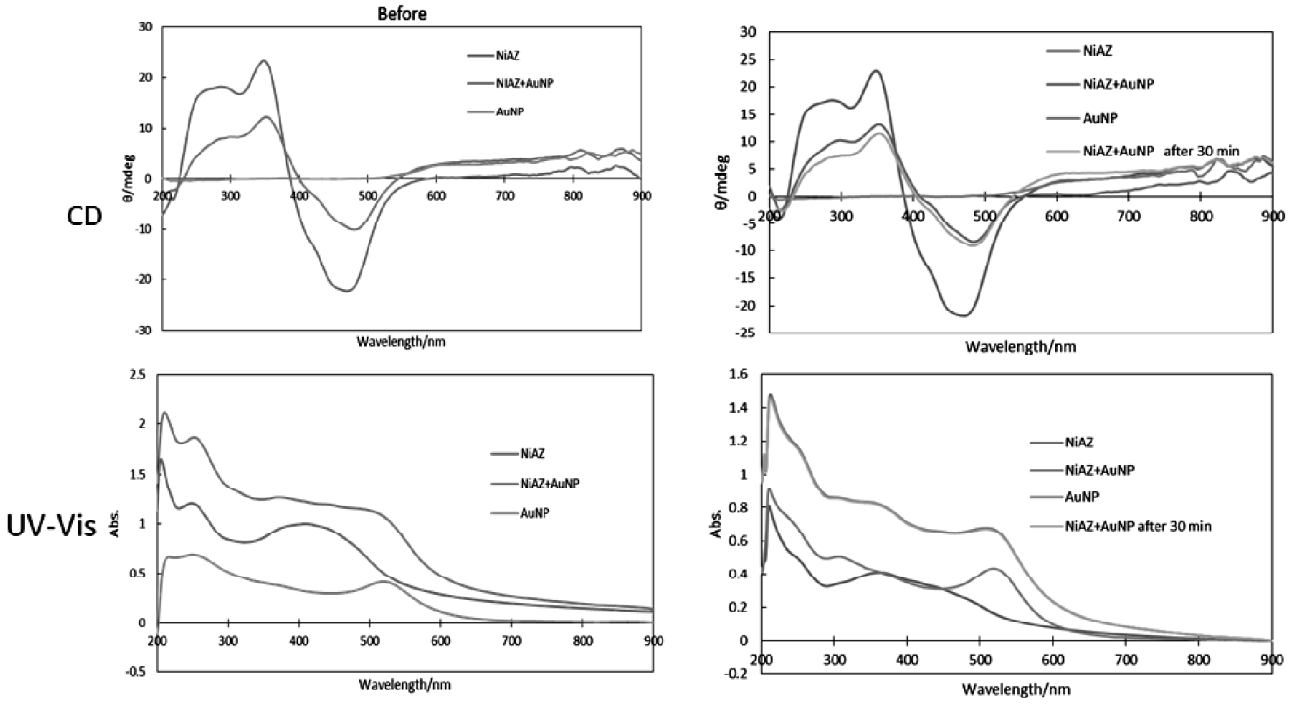

Fig. 8. CD and UV-Vis and CD spectra of **NiAZ** and/or AuNPs before and after irradiation of polarized UV light up to 30 min.

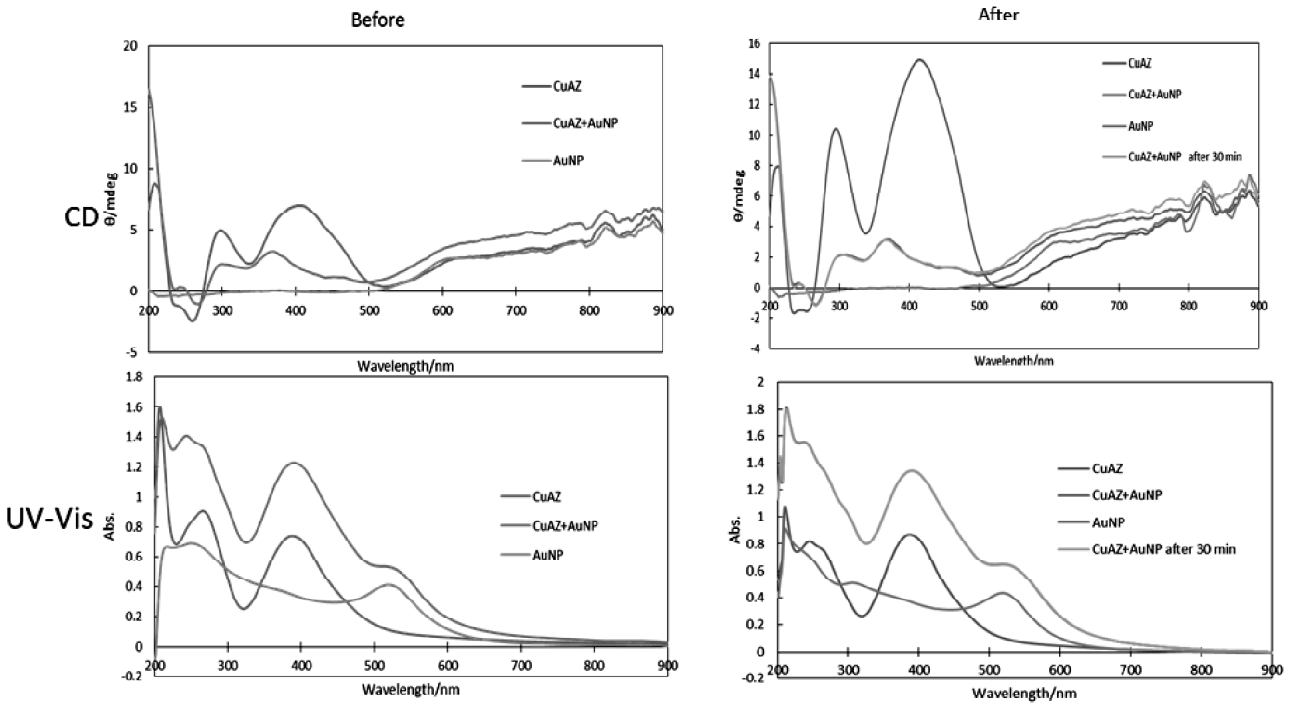

Fig. 9. CD and UV-Vis and CD spectra of **CuAZ** and/or AuNPs before and after irradiation of polarized UV light up to 30 min.

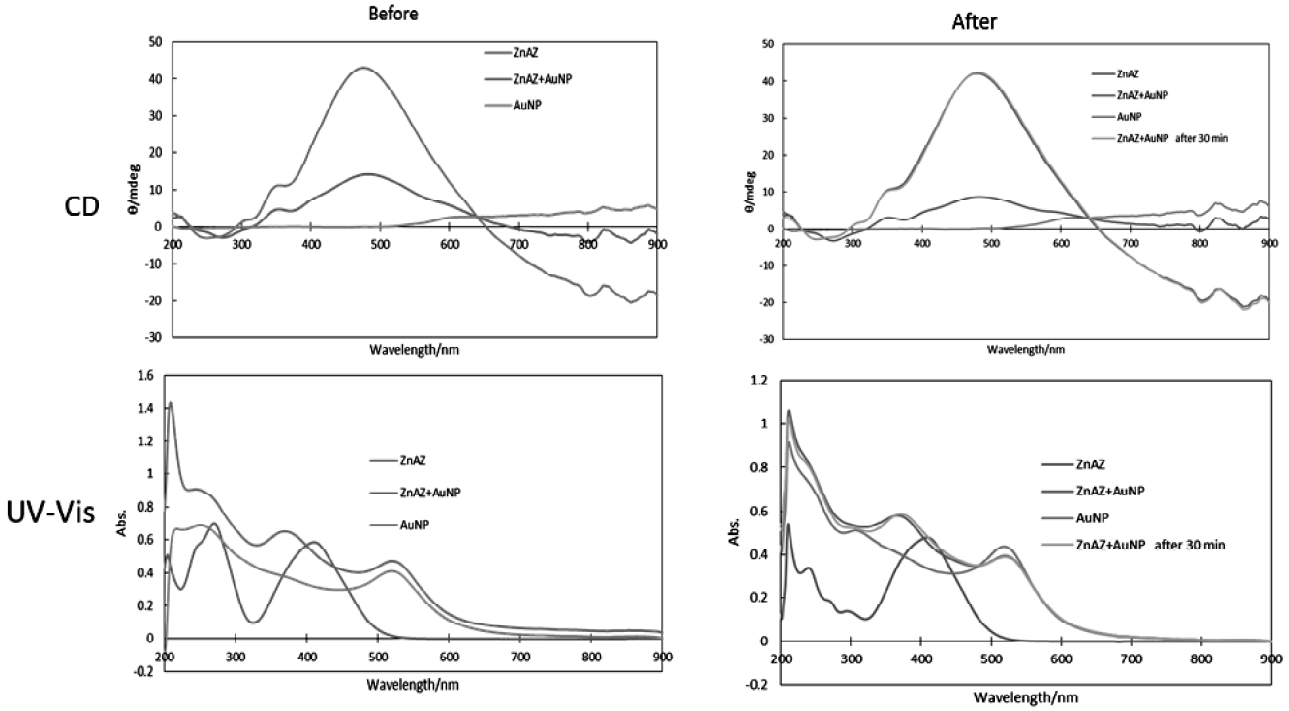

Fig. 10. CD and UV-Vis and CD spectra of **ZnAZ** and/or AuNPs before and after irradiation of polarized UV light up to 30 min.

the complex and AuNPs exhibit predominantly positive induced CD bands at about 500 nm. Additionally, after 30 min, it should be noted that mixed dispersions of the complex and AuNPs exhibit predominantly positive induced CD bands at about 500 nm. The bands are close to surface plasmon band of AuNPs.

Discussion :

The results of induced CD and their changes after linearly polarized UV light irradiation can be explained as summarized in Figs. 11–13 for **NiAZ**, **CuAZ**, and **ZnAZ** systems, respectively. Apparently, not only magnitude of dipole moment for the *trans* and *cis* forms of each complex but also molecular orientation of each complex on the surface of AuNPs may be concerned to the intensity of induced CD bands of surface plasmon region. Theoretically and experimentally, positively induced CD band can be observed parallel orientation of dipole-dipole interaction between chiral adsorbed molecules and AuNPs (as adsorbed by *trans* forms for all complexes systems and the *cis* form for **ZnAZ** systems)[27]. On the contrary, negatively induced CD can be expected for the opposite cases (the *cis* complexes systems for **NiAZ** and **CuAZ** systems). According to both experimental results of CD spectra and computational dipole moments of chiral complexes of discussed conditions, the expected situation in view of dipole-dipole interactions (essentially electromagnetic fields induced[28]) can be expressed as shown in Figs. 11–13. The changes of molecular orientation (resulted in magnitude of dipole moment predominantly) can be resulted from Weigert effect only after photoisomerization to the *cis* forms (resulted in directional change of dipole moment of chiral molecules). As for photo functional materials especially semiconductor systems[29,30], furthermore, potential application for solar cell materials can be expected reasonably.

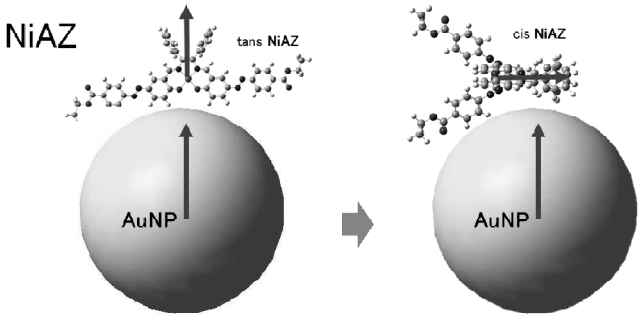

Fig. 11. Dipole moments of **NiAZ** and AuNPs before (left) and after (right) irradiation of polarized UV light.

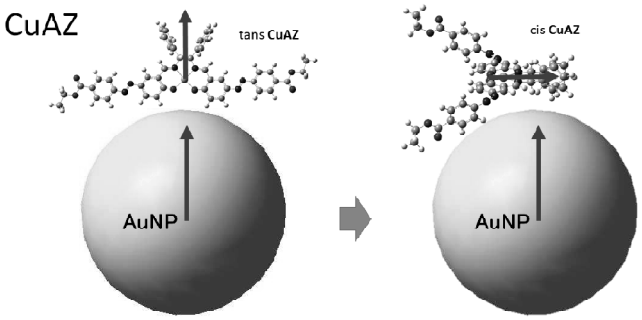

Fig. 12. Dipole moments of **NiAZ** and AuNPs before (left) and after (right) irradiation of polarized UV light.

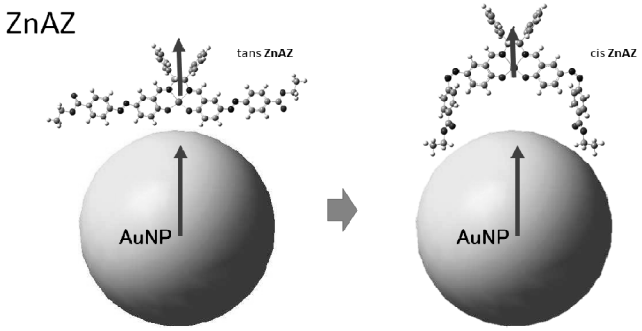

Fig. 13. Dipole moments of **NiAZ** and AuNPs before (left) and after (right) irradiation of polarized UV light.

Conclusions

In summary, we have prepared new chiral Schiff base Ni^{II}, Cu^{II} and Zn^{II} complexes having azobenzene moiety. For all complexes and AuNPs, induced CD could be observed around 500 nm. After linearly polarized UV light irradiation, features of induced CD spectra changed due to photoisomerization as well as Weigert effect of azobenzene moiety. TD-DFT computation could indicate differences of three metal com-

plexes due to coordination environment and could discuss differences in direction of dipole moment reasonably.

Acknowledgement

The computations were performed using Research Center for Computational Science, Okazaki, Japan. This XRD work was conducted at Advanced Characterization Nanotechnology Platform of the University of Tokyo supported by "Nanotechnology Platform" of the Ministry of Education, Culture, Sports, Science and Technology (MEXT), Japan.

Appendix A. Supplementary data

CCDC 1572657, 1572666, and 1572669 contain the supplementary crystallographic data for **NiAZ**, **CuAZ** and **ZnAZ**, respectively. These data can be obtained free of charge via http://www.ccdc.cam.ac.uk/conts/retrieving.html, or from the Cambridge Crystallographic Data Centre, 12 Union Road, Cambridge CB2 1EZ, UK; Fax : (+44) 1223-336-033; or E-mail : deposit@ccdc.cam.ac.uk.

References

1. M. C. di Gregorio, A. Ben-Moshe, E. Tirosh, L. Galantini and G. Markovich, *J. Phys. Chem. (C)*, 2015, **119**, 17111.
2. A. Ben-Moshe, A. Teitelboim, D. Oron and G. Markovich, *Nano Lett.*, 2016, **16**, 7467.
3. A. Ben-Moshe, S. G. Wolf, M. B. Sadan, L. Houben, Z. Fan, A. O. Govorov and G. Markovich, *Nature Commun.*, 2014, **5**, 4302.
4. S. Mackowski, S. Woermke, A. J. Maier, T. H. P. Brotosudarmo, H. Harutyunyan, A. Hartschuh, A. O. Govorov, H. Scheer and C. Braeuchle, *Nano Lett.*, 2008, **8**, 558.
5. N. Kimura, H. Nishizuru, Y. Aritake and T. Akitsu, *J. Chem. Chem. Eng.*, 2013, **7**, 390.
6. Y. Aritake, T. Nakayama, H. Nishizuru and T. Akitsu, *Inorg. Chem. Commun.*, 2011, **14**, 423.
7. S. Roy and M. A. Pericàs, *Org. Biomol. Chem.*, 2009, **7**, 2669.
8. B. T. Hogan, S. A. Dyakov, L. J. Brennan, S. Younesy, T. S. Perova, Y. L. Gun'ko, M. F. Craciun and A. Baldycheva, *Sci. Rep.*, 2017, **7**, 42120.
9. A. K. Visheratina, F. Purcell-Milton, R. Serrano-Garcia, V. A. Kuznetsova, A. O. Orlova, A. V. Fedorov, A. V. Baranov and Y. K. Gun'ko, *J. Mater. Chem. (C)*, 2017, **5**, 1692.
10. A. O. Govorov, Z. Fan, P. Hernandez, J. M. Slocik and R. R. Naik, *Nano Lett.*, 2010, **10**, 1374.
11. A. O. Govorov and Z. Fan, *ChemPhysChem.*, 2012, **13**, 2551.
12. A. Ben-Moshe, B. M. Maoz, A. O. Govorov and G. Markovich, *Chem. Soc. Rev.*, 2013, **42**, 7028.
13. C. Fleming, D.-L. Long, N. McMillan, J. Johnston, N. Bovet, V. Dhanak, N. Dadegaard, P. Loegerler, L. Cronin and M. Kadodwala, *Nature Nanotech.*, 2008, **3**, 229.
14. Y. Aritake, T. Takanashi, A. Yamazaki and T. Akitsu, *Polyhedron*, 2011, **30**, 886.
15. Y. Aritake and T. Akitsu, *Polyhedron*, 2012, **31**, 278.
16. A. Yamazaki and T. Akitsu, *RSC Adv.*, 2012, **2**, 2975.
17. K. Takahashi, S. Tanaka, M. Yamaguchi, Y. Tsunoda, T. Akitsu, M. Sugiyama, R. K. Soni and D. Moon, *J. Kor. Chem. Soc.*, 2017, **61**, 129.
18. M. Yamaguchi, Y. Tsunoda, S. Tanaka, T. Haraguchi, M. Sugiyama, S. Noor and T. Akitsu, *J. Indian Chem. Soc.*, 2017, **94**, 761.
19. O. A. Blackburn, B. J. Coe, J. Fielden, M. Helliwell, J. J. W. McDouall and M. G. Hutchings, *Inog. Chem.*, 2010, **49**, 9136.
20. M. J. Frisch, G. W. Trucks, H. B. Schlegel, G. E. Scuseria, M. A. Robb, J. R. Cheeseman, G. Scalmani, V. Barone, B. Mennucci, G. A. Petersson, H. Nakatsuji, M. Caricato, X. Li, H. P. Hratchian, A. F. Izmaylov, J. Bloino, G. Zheng, J. L. Sonnenberg, M. Hada, M. Ehara, K. Toyota, R. Fukuda, J. Hasegawa, M. Ishida, T. Nakajima, Y. Honda, O. Kitao, H. Nakai, T. Vreven, J. A. Montgomery (Jr.), J. E. Peralta, F. Ogliaro, M. Bearpark, J. J. Heyd, E. Brothers, K. N. Kudin, V. N. Staroverov, R. Kobayashi, J. Normand, K. Raghavachari, A. Rendell, J. C. Burant, S. S. Iyengar, J. Tomasi, M. Cossi, N. Rega, J. M. Millam, M. Klene, J. E. Knox, J. B. Cross, V. Bakken, C. Adamo, J. Jaramillo, R. Gomperts, R. E. Stratmann, O. Yazyev, A. J. Austin, R. Cammi, C. Pomelli, J. Ochterski, R. L. Martin, K. Morokuma, V. G. Zakrzewski, G. A. Voth, P. Salvador, J. J. Dannenberg, S. Dapprich, A. D. Daniels, O. Farkas, J. B. Foresman, J. V. Ortiz, J. Cioslowski and D. J. Fox, GAUSSIAN 09 (Revision A.1), Gaussian, Inc., Wallingford, CT, 2009.
21. Y. Mitsumoto, N. Sunaga and T. Akitsu, *Sci. Fed. J. Chem. Res.*, 2017, **1**, 1.

22. T. Hayashi, H. Shibata, S. Orita and T. Akitsu, *Eur. Chem. Bull.*, 2013, **2**, 49.
23. S. Orita and T. Akitsu, *Open Chem. J.*, 2014, **1**, 1.
24. R. Shoji, S. Ikenomoto, N. Sunaga, M. Sugiyama and T. Akitsu, *J. Appl. Sol. Chem. Model.*, 2016, **5**, 48.
25. M. Oshima, M. Matsuno, Y. Tsutsumi, N. Sunaga, T. Haraguchi and T. Akitsu, *Int. J. Org. Chem.*, 2017, **7**, 153.
26. M. Ito, T. Akitsu and M. A. Palafox, *J. Appl. Sol. Chem. Model.*, 2016, **5**, 30.
27. X. Duan, S. Yue and N. Liu, *Nanoscale*, 2015, **7**, 17237.
28. E. Hendry, R. V. Mikhaylovskiy, L. D. Barron, M. Kadodwala and T. J. Davis, *Nano Lett.*, 212, **12**, 3640.
29. A. O. Govorov, G. W. Bryant, W. Zhang, T. Skeini, J. Lee, N. A. Kotov, J. M. Slocik and R. R. Nail, *Nano Lett.*, 2006, **6**, 984.
30. J. Lee, A. O. Govorov and N. A. Kotov, *Nano Lett.*, 2055, **5**, 2063.